Received: 3 February 2021 | Revised: 17 May 2021 | Accepted: 19 May 2021
DOI: 10.1002/glia.24039

GLIA
WILEY

RESEARCH ARTICLE

Histamine triggers microglial responses indirectly via astrocytes and purinergic signaling

Pengfei Xia[1,2] | Francesca Logiacco[1,3] | Yimin Huang[1,2] | Helmut Kettenmann[1,4] | Marcus Semtner[1]

[1]Cellular Neurosciences, Max-Delbrück-Center for Molecular Medicine in the Helmholtz Association, Berlin, Germany

[2]Charité-Universitätsmedizin, Berlin, Germany

[3]Department of Biology, Chemistry, and Pharmacy, Freie Universität Berlin, Berlin, Germany

[4]Shenzhen Institute of Advanced Technology, Chinese Academy of Sciences, Shenzhen, China

Correspondence
Marcus Semtner, Cellular Neurosciences, Max-Delbrück-Center for Molecular Medicine in the Helmholtz Association, 13125 Berlin, Germany.
Email: marcus.semtner@mdc-berlin.de

Funding information
Einstein-Stiftung; Helmholtz-Gemeinschaft, Zukunftsthema "Immunology and Inflammation", Grant/Award Number: ZT-0027

Abstract

Histamine is a monoaminergic neurotransmitter which is released within the entire brain from ascending axons originating in the tuberomammillary nucleus in a sleep state-dependent fashion. Besides the modulation of neuronal firing patterns, brain histamine levels are also thought to modulate functions of glial cells. Microglia are the innate immune cells and professional phagocytes of the central nervous system, and histamine was previously shown to have multiple effects on microglial functions in health and disease. Isolated microglia respond only to agonists of the *Hrh2* subtype of histamine receptors (*Hrh*), and the expression of that isoform is confirmed by a metadata analysis of microglia transcriptomes. When we studied the effect of the histamine receptor isoforms in cortical and thalamic microglia by in situ *live* cell Ca^{2+} imaging using a novel, microglia-specific indicator mouse line, microglial cells respond to external histamine application mainly in a *Hrh1*-, and to a lower extent also in a *Hrh2*-dependent manner. The *Hrh1* response was sensitive to blockers of purinergic *P2ry12* receptors, and since *Hrh1* expression was predominantly found in astrocytes, we suggest that the *Hrh1* response in microglia is mediated by astrocyte ATP release and activation of *P2ry12* receptors in microglia. Histamine also stimulates microglial phagocytic activity via *Hrh1*- and *P2ry12*-mediated signaling. Taken together, we provide evidence that histamine acts indirectly on microglial Ca^{2+} levels and phagocytic activity via astrocyte histamine receptor-controlled purinergic signaling.

KEYWORDS
astrocyte, calcium, histamine, Hrh, microglia, phagocytosis

1 | INTRODUCTION

Histamine is a bioactive amine known to regulate many physiological processes in the periphery, such as allergic reactions, gastric acid secretion, and itch sensation (Thangam et al. (2018). In the central nervous system (CNS), histamine is synthesized by L-histidine decarboxylase (HDC)-expressing neurons which are localized in the tuberomammillary nucleus (TMN) from where they send axonal projections towards essentially all brain (Haas & Panula, 2003; Panula & Nuutinen, 2013). Histamine neurons are pacemakers that display

Helmut Kettenmann and Marcus Semtner should be considered shared senior author.

regular spontaneous firing patterns at low frequency which are correlated to sleep/wake rhythm with upregulation of histamine release during wakefulness (Vitrac & Benoit-Marand, 2017). Abnormalities in brain histamine release are increasingly appreciated as potential contributors to brain pathologies like Parkinson's disease, Huntington's disease, Alzheimer's disease, narcolepsy, and drug addiction (Panula & Nuutinen, 2013).

Histamine action is mediated by signaling downstream of the four mammalian histamine receptor isoforms (*Hrh1-Hrh4*) which are $G\alpha_q$ (*Hrh1*), $G\alpha_S$ (*Hrh2*), or $G\alpha_i$ (*Hrh3* and *Hrh4*) protein-coupled receptors. Recent transcriptomic and proteomic approaches suggest that there is—if at all—only bare expression of *Hrh4* in the central nervous system (Zhang et al., 2014). The predominant isoform in the brain is *Hrh3* which is mainly expressed by neurons and modulates the release of various neurotransmitters, including GABA and acetylcholine (Passani et al., 2000). Consistent with its abundance and strong impact on neurotransmitter release, *Hrh3* is involved in diverse brain functions, such as memory, cognition, appetite, and arousal. *Hrh1* and *Hrh2* are also expressed by neurons at low levels, however, previous gene expression studies and functional observations suggest that these subunits rather serve as modulators of glial functions. Particularly, *Hrh1*, which is the most abundant *Hrh* isoform in astrocytes, modulates various physiological and pathological activities of astrocytes upon brain histamine level changes including energy metabolism, neurotransmitter clearance, neurotrophic activity, and immune responses (Jurič et al., 2016).

Microglia are the resident immune cells of the CNS. Their physiological role is to protect the brain from infection and damage, to promote tissue repair and regeneration, and to modulate neurons and other glial cells by secretion of growth factors, cytokines, and other signal molecules (Wolf et al., 2017). In the healthy postnatal brain, microglia are characterized by a ramified morphology, that is, they have a relatively small soma ($\sim$10 μm) with cellular processes that branch off and arborize further more distantly from the soma within a defined territory, and they constantly scan their environment for potential insults (Kettenmann et al., 2011). Microglia are the professional phagocytes of the brain being able to eliminate entire cells or cellular substructures. Microglia recognize cells that undergo programmed cell death and they migrate to different regions of the CNS, usually right before or during the peak of programmed cell death (Wolf et al., 2017). The first report on histamine action on microglia was from Bader et al. (1994) who demonstrated via life cell Ca^{2+} imaging that only a subpopulation of primary cultured rat microglia is responsive to histamine application, a notion that was confirmed in a more recent study on freshly isolated and primary cultured mouse microglia (Pannell et al., 2014). Interestingly, the percentage of histamine-responding microglia dramatically increases upon LPS challenge, indicating that microglia can dynamically adjust their sensitivity to histamine, and suggesting that histamine action on microglia might be heterogeneous with regard to certain physiological and pathophysiological conditions. There are various controversial results of microglial *Hrh* expression and its functional impact. Indeed, histamine was reported to stimulate microglial phagocytic activity in vitro and in situ in a *Hrh1*-dependent manner (Rocha et al., 2016). Another study demonstrated an inhibitory effect of histamine on microglial phagocytosis in vitro via *Hrh3* (Iida et al., 2015). Further controversy is about microglial migration which was shown to be accelerated by histamine in a *Hrh4*-dependent fashion and in another study inhibited by *Hrh1* and *Hrh2* (Apolloni et al., 2017). In the present study, we used a novel microglia-specific Ca^{2+} indicator mouse model to investigate microglial Ca^{2+} elevations upon histamine and *Hrh*-specific agonists in cortex and thalamus. We provide evidence for functional *Hrh2*, but not *Hrh1*, *Hrh3*, or *Hrh4* expression on microglia and demonstrate that *Hrh1* in astrocytes and microglial *P2ry12* are involved in histamine action on microglia in situ.

2 | MATERIALS AND METHODS

2.1 | Animals

This study was carried out at the Max Delbrück Center for Molecular Medicine (MDC) in strict accordance with the guidelines of the European Communities Council Directive for care of laboratory animals (86/609/EEC) and of the State of Berlin's Office for Health and Social Affairs (Landesamt für Gesundheit und Soziales, LaGeSo), as well as internal MDC guidelines. Experimental protocols were approved under license (X9005/18, X9023/12, A0376/17). Animals were bred and maintained at the MDC animal facility in a temperature- and humidity-controlled environment with a 12 h light–dark cycle and ad libitum access to food and water. The mouse strains Csf1R-2A-GCaMP6m and Csf1R-2A-mCherry-2A-GCaMP6m are novel, microglia-specific calcium indicator lines which are described in another paper from our lab (Logiacco et al., in press). hGFAP-mRFP transgenic mice express the red fluorescent protein (mRFP) in astrocytes under control of the promotor for human glial fibrillary acidic protein (GFAP) (Hirrlinger et al., 2005). We pooled male and female mice in all experiments.

2.2 | Chemicals

The following substances were used in the present study: histamine dihydrochloride (Sigma-Aldrich; 100 μM), 2-pyridylethylamine dihydrochlid (2-PEA; R&D Systems; 100 μM), amthamine (Enzo; 10 μM), α-methylhistamine (αMH; Biomol; 1 μM), VUF 10460 (Biomol; 10 μM), cetirizine (Sigma-Aldrich; 10 μM), Tiotidine (R&D Systems; 10 μM), carcinine (Sigma-Aldrich; 10 μM),, AR-C69931 tetrasodium salt (Tocris, Bio-Techne GmbH, Wiesbaden-Nordenstadt; 1 μM). All chemicals were obtained as powder and initially stock-diluted at a 1,000 fold concentration in DMSO or H_2O.

2.3 | Acute brain slice preparation

Acute cortical brain slices from adult male and female C57BL/6, Csf1R-2A-GCaMP6m or Csf1R-2A-mCherry-2A-GCaMP6m mice

(P40–P90) were prepared as previously described (Boucsein et al., 2003). In brief, adult mice were killed by cervical dislocation. After the brain was extracted, the cerebellum and the olfactory bulbs were gently removed and transferred to ice-cold slicing solution (230 mM sucrose, 26 mM $NaHCO_3$, 2.5 mM KCl, 1.25 mM NaH_2PO_4, 10 mM $MgSO_4$, 0.5 mM $CaCl_2$, 10 mM D-glucose; pH 7.4; saturated with carbogen: 95% O_2, 5% CO_2) to generate 140 μm (phagocytosis assay) or 250 μm (Ca^{2+} imaging) thick coronal slices using a vibratome (HM650V, Thermo Scientific). Slices were immediately transferred into artificial cerebrospinal fluid (ACSF): 134 mM NaCl, 26 mM $NaHCO_3$, 2.5 mM KCl, 1.26 mM K_2HPO_4, 1.3 mM $MgCl_2$, 2 mM $CaCl_2$, 10 mM D-glucose; pH 7.4 which was saturated with carbogen (95% O_2, 5% CO_2) at room temperature. The brain slices were kept in ACSF at least 1 h until further treatment.

2.4 | Preparation of freshly isolated microglia

Microglia from adult C57BL/6 mice (P49–P90) were acutely isolated and purified for calcium imaging using magnetic-activated cell sorting (MACS) as described previously (Nikodemova & Watters, 2012). Briefly, adult mice were sacrificed by transcardial perfusion with ice-cold phosphate-buffered solution (PBS) under deep anesthesia to remove the blood. The brain was removed and only the cortex was dissected into Miltenyi Biotec adult brain Dissociation Kit (Trypsin) and dissociated in the gentleMACS Octo Dissociator with heaters (Miltenyi Biotech) for 30 min. After dissociation, the suspension was passed through a MACS SmartStrainer (70 μm) followed by centrifugation for 1 min at 300 g and 4°C to obtain a single cell suspension. The cell suspension was then homogenized and resuspended in debris removal solution (Miltenyi Biotech). A layer of PBS was very gently applied on top and centrifuged at 3000*g*, 4°C for 10 min with full acceleration and full brake. The cells were washed and resuspended in MACS-buffer (PBS, 0.5% bovine serum albumin, 2 mM EDTA) and stained with CD11b magnetic Microbeads (Miltenyi Biotech) at 4°C for 15 min. Labeled CD11b-positive cells (microglia) within the large-sized MACS column were then flushed out and plated onto glass coverslips, followed by incubation in DMEM (Invitrogen, Karlsruhe, Germany) medium for at least 2 h to allow adherence. Ca^{2+} imaging was subsequently carried out as described below.

2.5 | Calcium imaging

Acutely isolated microglial cells were plated on glass coverslips. After 2 h, adhered microglia were incubated for 40 min with 5 μM Fluo-4/AM (Invitrogen) in standard extracellular solution (150 mM NaCl, 5.4 mM KCl, 0.98 mM $MgCl_2$, 1.97 mM $CaCl_2$, 10 mM HEPES, and 10 mM glucose; pH 7.4) at room temperature. Acute brain slices from Csf1R-2A-GCaMP6m mice were only maintained in carbogenized ACSF at RT, while slices (250 μm) from C57/Bl6 mice were generated and loaded with 10 μM Fluo4/AM for 1 h at 37°C to stain astrocytes.

Coverslips or brain slices were transferred into a recording chamber constantly perfused with standard extracellular solution (isolated microglia) or carbogenized ACSF (brain slices). The perfusion system was equipped with a perfusion pencil which allowed instant and local application of the test substances, as well as 1 mM ATP (Adenosine-Triphosphate) applied at the end of every recording as control. The flow of the perfusion system was adjusted to 0.5–0.6 ml/min. Before live cell Ca^{2+} imaging, each brain slice/coverslip was first examined using a 5X objective and bright field illumination. For Ca^{2+} recordings, we used a ×20 objective (Carl Zeiss Microscopy GmbH), a Zyla 5.5 camera (Oxford Instruments), a light-emitting diode illuminator (pE-4,000, CoolLED, Andover, UK) and a standard EGFP filter set. An EPC9 amplifier (HEKA) and TIDA 5.25 software (HEKA) were used to trigger fluorescence excitation and image acquisition. To monitor Ca^{2+} level changes over time, images were taken at a rate of 1 frame per second and an exposure time of 100 ms. For experiments at 37°C, we used an inline heater (Warner Instruments Corp.).

For 2-Photon imaging, we used a custom-built 2-photon microscope consisting of an BX61WI microscope stage (Olympus) equipped with a ×40 water immersion objective placed on a PD72Z4CA piezo drive (Physik Instrumente), a Chameleon Ultra II laser (Coherent) and GaAsP photomultipliers (Thorlabs). The GCaMP6m protein was excited at a wavelength of 940 nm. Movies were acquired at a sampling rate of one 3D image per second, whereas each 3D image covered seven fields of 160 × 160 μm with a z distance of 2 μm (i.e., total z distance: 40 μm). ThorImage 8.0 was used to drive the image acquisition during calcium imaging experiments. For offline analysis, each 3D image was subjected to a maximum intensity projection to obtain a 2D movie by using a custom-built procedure in IGOR Pro 6.37 (WaveMetrics). Calcium imaging movies were analyzed using a home-made algorithm in Igor Pro 6.37 (WaveMetrics). For analysis, cell somata which were visible in the presence of ATP at the end of each experiment were selected as ROIs, and the mean relative fluorescence intensity for each ROI and frame was determined to display changes in Ca^{2+} levels over time for each cell. This means that only ATP-responding microglia/astrocytes were taken into the subsequent analysis. Intracellular Ca^{2+} elevations were counted as "responsive" upon application of a substance when the Ca^{2+} response amplitude exceeded a level three times (microglia) or five times (astrocytes) the *SD* from the baseline that was obtained in the 60 s immediately before application. We averaged the cellular response rates from each slice to obtain one "*n*" for the subsequent statistical analysis. Recordings with less than five microglia in the view field were excluded from analysis. For the analysis of amplitudes and kinetics of microglial Ca^{2+} responses as well as for averaging histamine responses in the figures (stated as "responding"), we used only "responding" events and excluded non-responders.

2.6 | In situ phagocytosis assay

Phagocytosis assay in acute cortical or thalamic brain slices was conducted as previously described (Wendt et al., 2017). Briefly, coronal brain slices from C57/Bl6 mice were generated and maintained for

2 h at RT in ACSF to recover from the slicing procedure (see above). Subsequently, slices were incubated at 37°C for 1 h with latex beads (4.5 μm diameter, Polysciences, Hirschberg Germany), either only in ACSF or together with the specified histamine or isoform-specific agonists and antagonists; then washed three times in 0.1 M PBS (20 min), fixed with 4% paraformaldehyde for 1 h for subsequent staining and again washed three times in 0.1 M PBS (20 min each). For staining, slices were incubated for 4 h at room temperature in a permeabilization buffer containing 2% Triton X-100 (Carl Roth), 2% bovine serum albumin (Carl Roth), 10% normal donkey serum (EMD Millipore) in 0.1 M PBS (pH 7.4) and then overnight incubated with a goat anti-Iba1 antibody (1:600; clone #5076 Abcam) in dilution buffer (1:10 of permeabilization buffer in 0.1 M PBS) at 4°C. On the next day, slices were incubated for 2 h with the secondary antibody donkey anti-goat Alexa Fluor 647 (1:250; Dianova). After washing, the slices were mounted on glass slides with Aqua Polymount mounting medium (Polysciences). Confocal laser scanning microscopy was performed on a Leica TCS SPE confocal microscope (Leica) using a ×20 oil immersion objective. We acquired 21 μm thick z-stacks at 1.05 μm intervals beginning from the surface of the slice.

Data analysis to assess microglial phagocytic activity was performed using Imaris 6.3.1 (Bitplane). The Iba1-positive volumes of high-resolution SPE confocal microscopy stacks were 3D surface rendered using a software-internal threshold value of 40 AU and a background subtraction (software-internal parameters: 1–3 times, ~90 μm each). Microspheres were detected as spots and counted. All beads having their center located within a given rendered Iba1 volume were considered to be phagocytosed by microglia. The phagocytic index was calculated as: $n_{PM}*10^4/V_{Iba1}$ (n_{PM} is the total number of phagocytosed microspheres and V_{Iba1} is the Imaris-rendered volume of Iba1 fluorescence in μm^3). Igor Pro 6.37 (WaveMetrics) and Prism 7 (GraphPad Software) were used for subsequent statistical analysis.

2.7 | Metadata analysis

The cell-type-specific expression of *Hrh* isoforms was obtained directly from the website www.brainrnaseq.org. Single FPKM values were compiled in IGOR Pro 6.37 and plotted as heat map (Figure S1A; Zhang et al., 2014). For looking into the brain region-specific microglial RNAseq dataset at different ages (Grabert et al., 2016), the normalized data set GSE62420 was downloaded from the GEO site (https://www.ncbi.nlm.nih.gov/geo/), and FPKM values of each sample were normalized to the expression of *Hprt* for a proper comparison between different brain regions. *Hrh* and *P2ry12* values were finally compiled in IGOR Pro 6.37 and plotted as heat map. For *Hrh* and *P2ry12* expression in single microglia (Tabula Muris Consortium, 2018), we utilized the online tools on https://tabula-muris.ds.czbiohub.org/ and exported the resulting plots.

2.8 | Statistical analysis

All data represent the percentage of microglia responding in each brain region from at least three animals per experimental condition. We applied the Kruskal-Wallis followed by a Dunn's multiple comparison test to calculate significance levels between data sets. Data are given as median ± 25%/75% percentile. Statistical significance levels are represented as n.s.: $p > .05$; *: $p < .05$; **: $p < .01$; ***: $p < .001$.

3 | RESULTS

3.1 | Microglial histamine responses are mediated by Hrh2 receptors

Microglia were previously shown in vitro to functionally express histamine receptors that mediate downstream cytosolic Ca^{2+} elevations (Pannell et al., 2014). We revisited these findings and determined histamine responses in freshly isolated cortical microglia from C57/Bl6 mice which were loaded with Fluo4/AM to indicate intracellular Ca^{2+} level changes (Figure 1a,b). ATP (1 mM) was applied at the end of each recording and only ATP-responding cells were considered for the subsequent analysis. As microglia are known to display spontaneous Ca^{2+} elevations (Korvers et al., 2016), we first determined the probability of spontaneous events within a minute before histamine application which was observed in 1.13 ± 0/3.39% of the cells ($n = 3{,}028$ isolated cells, 54 recordings, 11 mice). In accordance with our published data set, a subpopulation (5.88 ± 2.98/8.00%; $n = 502$ cells, 15 recordings, 4 mice) of these microglial cells responded to histamine which was a significantly higher rate than spontaneous Ca^{2+} elevations before histamine application ($p = .0021$). Microglial Ca^{2+} responses to histamine had a peak of 0.72 ± 0.16 relative to the responses upon ATP; they were transient and completely reversed to background levels upon wash out.

In the mammalian genome, there are four known histamine receptor isoforms (Hrh1-4; Passani et al., 2000). In an attempt to identify the receptor isoform responsible for microglial histamine responses, we used *Hrh* isoform-specific agonists. As shown in Figure 1c,d, freshly isolated microglia selectively responded to the *Hrh2*-specific agonist amthamine (10 μM). 4.17 ± 2.38/11.83% of the ATP-responding isolated microglia displayed amthamine-evoked Ca^{2+} elevations ($n = 1{,}345$ cells, 25 recordings, 7 mice) which was similar to the histamine-responding population (5.88 ± 2.98/8.00%; $p = .9999$) and significantly more than the level of spontaneously active cells ($p = .0016$). *Hrh1* activation by 2-pyridylethylamine dihydrochlid (2-PEA; 100 μM) did, however, not stimulate Ca^{2+} elevations in freshly isolated microglia as the response rate was similar to basal activity (2 ± 0.37/3.75%; $n = 962$ cells, 15 recordings, 5 mice; $p = .9999$). There was also no response to *Hrh3* and *Hrh4* activation by α-Methylhistamine (αMH; 1 μM) and VUF 10460 (VUF; 10 μM), respectively (Figure 1d). We therefore conclude that microglia express *Hrh2* receptors which mediate intracellular Ca^{2+} elevations upon histamine application. This conclusion is strongly supported by previously published transcriptomic expression profiles of microglia and other brain cell types. A meta-analysis of several data sets (Figure S1) revealed that indeed *hrh2* is the predominant isoform in microglia whereas *hrh1* is mainly expressed by astrocytes and *hrh3* by neurons (Zhang et al., 2014). Specific expression of *hrh2* in microglial

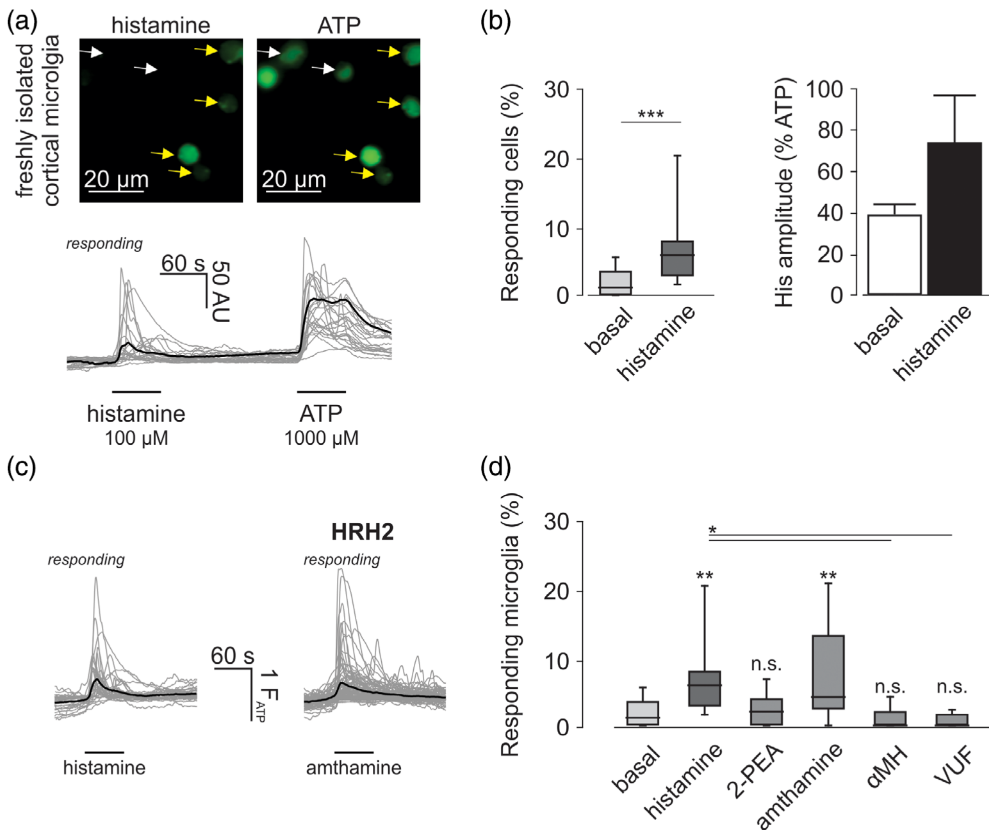

FIGURE 1 Freshly isolated cortical microglia respond to histamine via *Hrh2* activation. (a) *Top*, representative images from live-cell recordings on adult isolated microglial cells in the presence of histamine (left) and ATP (right). Isolated microglia were obtained from C57/Bl6 cortex via MACS (CD11b) and loaded with Fluo4/AM before recordings. Images were generated by subtraction of the movie frames before substance application from frames in the presence. Histamine-responding microglia are indicated with a yellow arrow, non-responding microglia with a white arrow. *Bottom*, overlay of intracellular Ca^{2+} responses from cortical histamine-responding microglia. The black trace is the average response of all responding cells (gray). (b) *Left*, percentage of freshly isolated microglia responding spontaneously or upon histamine application. *Right*, Average amplitudes of microglial histamine responses normalized to the amplitude of ATP responses. (c) Overlay of intracellular Ca^{2+} responses from microglia in response to histamine (100 μM, left) and amthamine (*Hrh2* agonist; 10 μM, right). The black trace is the average response of all responding cells (gray). (d) Summary of microglia Ca^{2+} responses upon histamine (100 μM), 2-PEA (*Hrh1* agonist; 100 μM), amthamine (*Hrh2* agonist; 10 μM), α-methylhistamine (αMH; *Hrh3* agonist; 1 μM) or VUF 10460 (VUF; *Hrh4* agonist; 10 μM) and under basal conditions. Note that only *Hrh2* activation evoked microglial Ca^{2+} responses similar to histamine. Significance statement above the bars is from comparison against basal conditions. Box Plots indicate the median (black line) as well as the 25%–75% (box) and 10%–90% (whiskers) percentiles. Statistical significance was tested by a Kruskal-Wallis test followed by Dunn's multiple comparisons test and is indicated as followed: n.s., $p \geq .05$; *$p \leq .05$; **$p \leq .01$, ***$p \leq .001$. Number of mice/experiments/cells: N(basal) = 11/54/3028; N(histamine) = 8/15/502; N(2-PEA) = 5/15/962; N(amthamine) = 7/25/1345; N(αMH) = 2/5/120; N(VUF) = 1/4/144

cells was also confirmed in many other transcriptomic data sets including the one provided by Grabert et al. (2016); Figure S1B), the Tabula Muris Consortium (2018); Figure S1C), Bowman et al. (2016)) and Sala Frigerio et al. (2019)). Taken together, both transcriptomic analysis and live cell investigation of isolated microglia support the notion that *Hrh2* is the only histamine receptor isoform expressed intrinsically in microglial cells and mediates microglial Ca^{2+} responses upon histamine stimulation.

3.2 | A subpopulation of microglia responds to histamine in different brain regions

We applied our novel transgenic Ca^{2+} indicator mouse model (Logiacco et al., in press), Csf1R-2A-GCaMP6m to test for microglial histamine responses in situ. In this mouse model, a transgenic *gcamp6m* cassette preceded by a 2A sequence is introduced right before the stop codon of the endogenous *Csf1r* gene, leading to the expression of the Ca^{2+} indicator protein GCaMP6m specifically in microglia. Acute cortical brain slices were generated from adult (P40–P90) male and female indicator mice to monitor microglial intracellular Ca^{2+} responses upon bath application of histamine (100 μM) using live-cell imaging (Figure 2a). In accordance to our observations in Logiacco et al. (in press), the intensity of the GCaMP6m fluorescence under basal conditions was very low in this mouse model, and the fluorescence within microglia was nearly indistinguishable from background fluorescence. Microglial cells undergoing intracellular Ca^{2+} elevations, however, display strong enhancements in GCaMP6m fluorescence (see Figure 1a). Like in vitro experiments (see Figure 1),

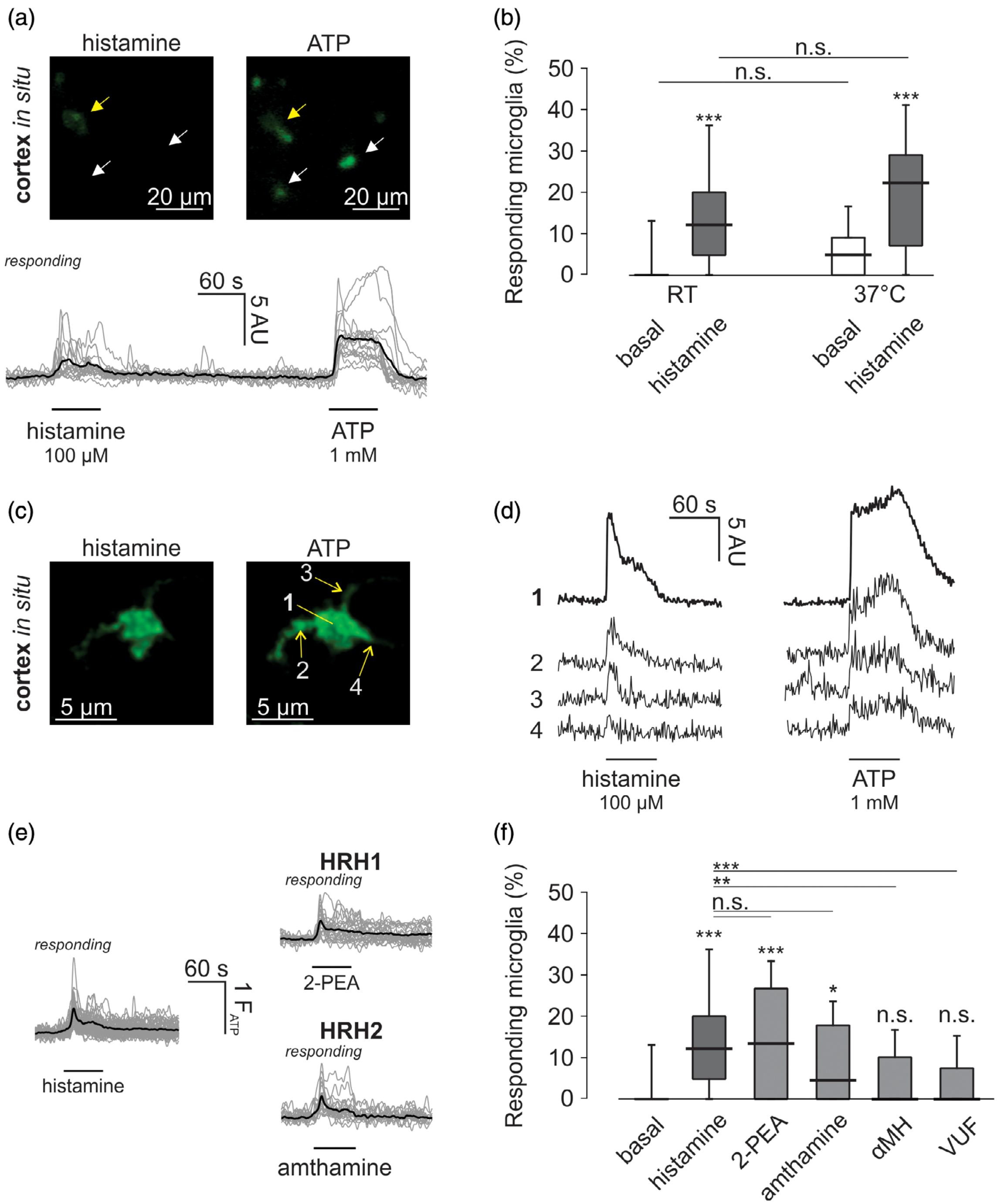

FIGURE 2 Cortical microglia in situ respond to histamine via *Hrh1* and *Hrh2*. (a) *Top*, representative microglial cells during live cell recordings from adult cortical brain slices in the presence of histamine (left) and ATP (right). Images were generated by subtraction of the movie frames before substance application from frames in the presence. Histamine-responding microglia are indicated with a yellow arrow, non-responding microglia with a white arrow. *Bottom*, overlay of intracellular Ca^{2+} responses to histamine from cortical microglia. The black trace is the average response of all responding cells (gray). (b) Summary of the percentage of histamine-responding microglia in situ (*left*). Average amplitudes of microglial histamine responses normalized to the amplitude of ATP responses (*right*). (c). Representative microglial cell during a 2-photon live-cell recording from an adult cortical brain slice in the presence of histamine (left) and ATP (right). Images were generated by subtraction of the movie frames before substance application from frames in the presence. Note that only proximal processes responded to ATP and histamine. (d) Intracellular Ca^{2+} responses from cortical histamine-responding microglia. Regions of interest of the traces are indicated by arrows in (c). (e) Overlay of intracellular Ca^{2+} responses from in situ cortical microglia responding to histamine, a *Hrh1*- (2-PEA, 100 μM) and a *Hrh2*- (Amthamine; 10 μM) specific agonist. Black traces indicate the average response of all responding cells (gray). (f) Summary of the percentage of responding microglia from experiments shown in (c), including those with *Hrh3*- (α-methylhistamine; 10 μM) and *Hrh4*- (VUF 10460; 10 μM) specific agonists. Box Plots indicate the median (black line) as well as the 25%–75% (box) and 10%–90% (whiskers) percentiles. Statistical significance was tested by a Kruskal Wallis test followed by Dunn's multiple comparisons test and is indicated as followed: n.s., $p \geq .05$; *$p \leq .05$; **$p \leq .01$, ***$p \leq .001$. Number of mice/experiments/cells: N(basal) = 16/143/1296; N(histamine) = 11/45/747; N(2-PEA) = 4/24/167; N(amthamine) = 4/24/184; N (αMH) = 6/29/346; N(VUF) = 6/30/364; N(basal 37°C) = 4/19/261; N(histamine 37°C) = 4/21/272

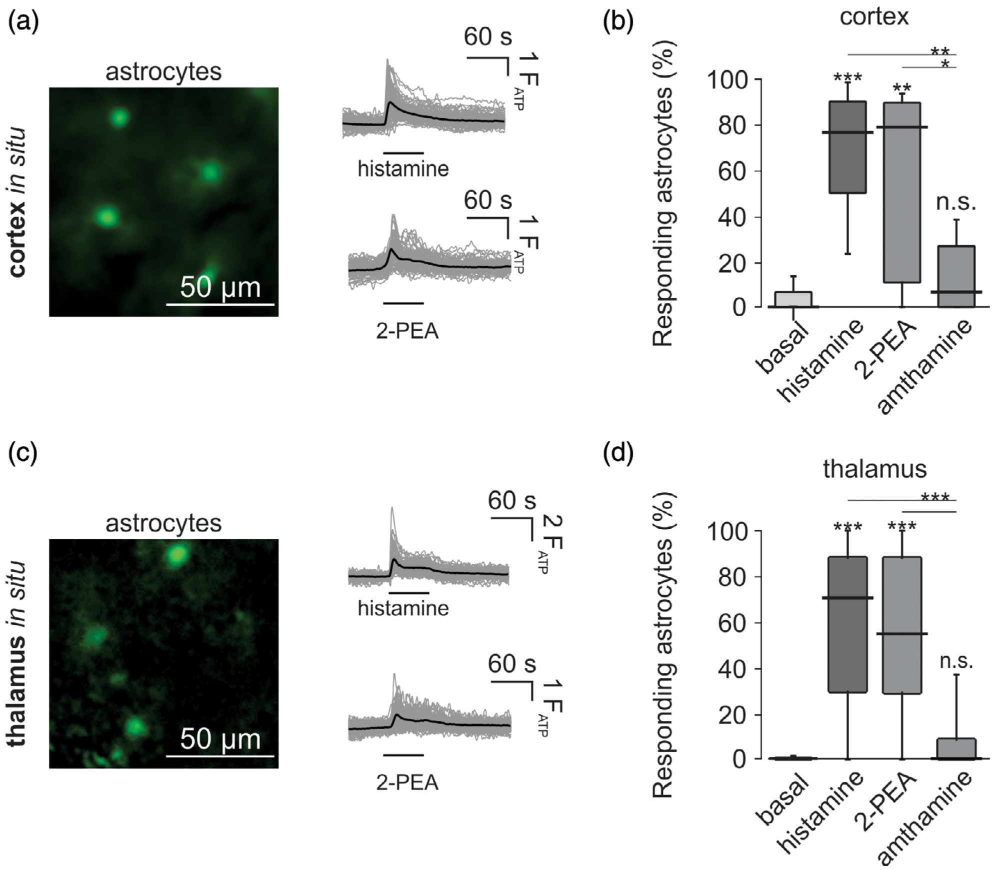

FIGURE 3 Astrocytes in cortex and thalamus respond to histamine via *Hrh1*. (a) Representative astrocytes from cortex during live cell imaging recordings from adult brain slices in the presence of the *Hrh1*-specific agonist 2-PEA. Slices were loaded with 10 μM Fluo4/AM to record astrocytic Ca^{2+} level changes. Images were generated by subtraction of the movie frames before substance application from frames in the presence. Traces on the right show the overlay of intracellular Ca^{2+} responses from cortical histamine- or 2-PEA-responding astrocytes. Black traces indicate the average response of all responding cells (gray). (b) Summary of the percentage of histamine-, 2-PEA (*Hrh1* agonist)- and amthamine (*Hrh2* agonist)- responding astrocytes in cortical slices. (c) and (d) Same as (a) and (b) but data were obtained from in situ recordings in the thalamus. Box plots indicate the median (black line) as well as the 25%–75% (box) and 10%–90% (whiskers) percentiles. Statistical significance was tested by a Kruskal Wallis test followed by Dunn's multiple comparisons test and is indicated as followed: n.s., $p \geq .05$; *, $p \leq .05$; **, $p \leq .01$; ***, $p \leq .001$. Number of mice/experiments/cells: N(Cx basal) = 3/10/124; N(Cx histamine) = 4/11/143; N(Cx 2-PEA) = 3/10/124; N(Cx amthamine) = 3/11/129; N(Tha basal) = 4/47/457; N(Tha histamine) = 2/16/168; N(Tha 2-PEA) = 2/13/133; N(Tha amthamine) = 4/16/147

histamine in situ also induced Ca^{2+} elevations only in a subset of microglia (Figure 2b) with 12.1 ± 5.3%/20.0% of ATP-responding cells being also responsive for histamine ($n = 747$ cells, 45 slices, 11 mice). The subpopulation of histamine-responding microglia was significantly larger in situ than in vitro ($p = .0105$). There were no significant differences between microglial responses from male and female brain slices ($p = .0657$). Histamine responses were often biphasic with a fast initial, transient rise and a second, sustained phase which reversed to baseline Ca^{2+} levels upon wash out of histamine (Figure 2a). The peak amplitude of the initial intracellular Ca^{2+} rise was on average 57.7 ± 5.9% of the ATP-evoked Ca^{2+} elevation. We also quantified the percentage of cells that responded randomly within a 60 s period before histamine application. 0.0 ± 0.0/0.0% of the ATP-responding microglia displayed this spontaneous activity indicating that histamine induced a significant response over baseline activity ($p < .0001$). There were no significant differences in basal ($p = .3226$) or histamine ($p > .9999$) responses when experiments were performed at 37°C (Figure 2b). We next investigated if microglial histamine responses are also abundant in processes. As shown in Figure 2c,d, Ca^{2+} responses upon ATP application were, if at all, only found in the proximal parts of microglial processes. On average, 1.46 ± 0.31 (proximal) processes per microglia responded to ATP. We quantified the process Ca^{2+} signals upon histamine in microglia that displayed a somatic histamine response and found that the majority of ATP-responding processes (73.7%) did also respond to histamine. These data demonstrate that microglial Ca^{2+} responses to ATP and histamine are much more pronounced in somata than processes.

We next addressed the question if there is brain region-specific heterogeneity in microglial histamine responses and performed in situ live cell recordings in hippocampus, striatum, thalamus, and corpus callosum. As shown in Figure S2, microglia responded also in these brain regions upon application of 100 μM histamine. The proportion of histamine-responding microglia was comparable to cortex in hippocampus (7.3 ± 0.0/20.0%; $n = 320$ cells, 46 slices, 10 mice; $p > .9999$),

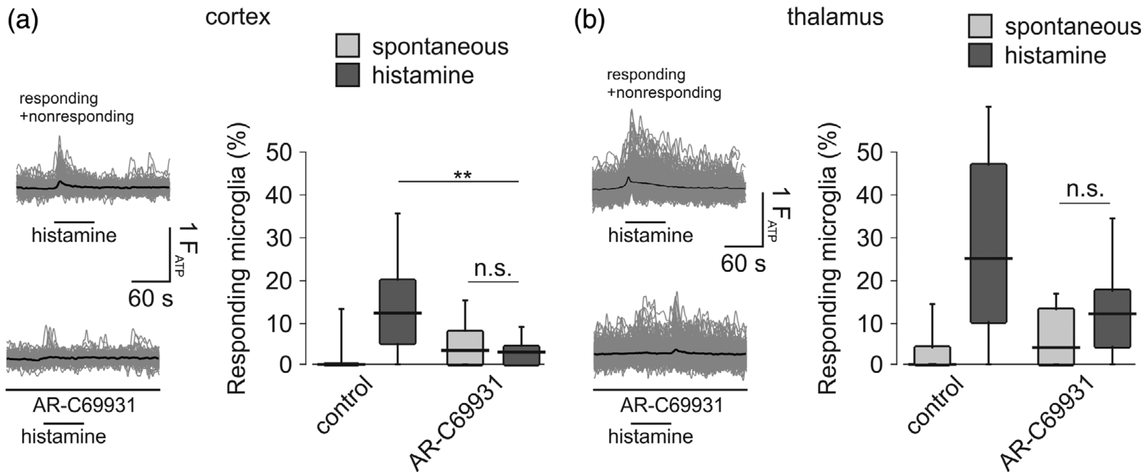

FIGURE 4 Histamine-evoked microglial Ca^{2+} responses depend on *P2ry12*. (a) *Left*, overlay of intracellular Ca^{2+} responses from in situ cortical microglia responding to histamine in the presence or absence of the *P2ry12* inhibitor AR-C69931 (1 μM). Black traces indicate the average response of all responding cells (gray). Note that unlike in the other figures, both responding and non-responding traces are shown in these plots. *Right*, summary of the percentage responding microglia from experiments shown in (a). (b) Same as (a) but data were obtained from thalamic microglia in situ. Box plots indicate the median (black line) as well as the 25%–75% (box) and 10%–90% (whiskers) percentiles. Statistical significance was tested by a Kruskal Wallis test followed by Dunn's multiple comparisons test and is indicated as followed: n.s., $p \geq .05$; *, $p \leq .05$; **, $p \leq .01$, ***$p \leq .001$. Number of mice/experiments/cells: N(Cx basal) = 16/143/1296; N(Cx histamine) = 11/45/747; N(Cx ARC basal) = 4/22/555; N(Cx ARC histamine) = 4/23/590; N(Tha basal) = 39/229/2250; N(Tha histamine) = 13/47/613; N(Tha ARC basal) = 4/20/393; N(Tha ARC histamine) = 4/16/147

striatum (0.0 ± 0.0/12.5%; n = 238 cells, 39 slices, 12 mice, p = .0904), thalamus (25.0 ± 11.9/45.8%; n = 253 cells, 37 slices, 12 mice; p = .1611) and corpus callosum (22.5 ± 5.8/52.1%; n = 323 cells, 36 slices, 12 mice; p = .3635). Significant differences were found between hippocampus and striatum in which microglia responded to a lesser extend to histamine than in thalamus (p = .0023 vs. HC; p < .0001 vs. Str) and in the corpus callosum (p = .0105 vs. HC; p < .0001 vs. Str).

Taken together, we conclude from these experiments that a subpopulation of microglia responds to histamine in vitro and in situ, and that the percentage of histamine-responding microglia varied among different brain regions.

3.3 | Microglial histamine responses in situ are mediated by Hrh1 and Hrh2

We next performed in situ Ca^{2+} recordings on cortical microglia using *Hrh* isoform-specific agonists (Figure 2c,d). Surprisingly, application of the *Hrh1*-specific agonist 2-pyridylethylamine dihydrochlid (2-PEA; 100 μM) led to microglial Ca^{2+} elevations in 13.4 ± 0.0/25.6% of cortical microglia (n = 184 cells, 24 slices, 4 mice) which was not significantly different to the response rate upon 100 μM histamine (p > .9999). Amthamine (10 μM), which specifically activates *Hrh2* receptors, evoked also Ca^{2+} responses in 4.6 ± 0.0/17.1% of the microglia (n = 184 cells, 24 slices, 4 mice) which was still higher than spontaneous activity (p = .0440) and not different from histamine (p = .4190). The *Hrh3*- and *Hrh4*-specific agonists αMH (1 μM) and VUF 10460 (10 μM) did not evoke Ca^{2+} responses in cortical microglia.

We aimed at verifying these results in another brain region and investigated microglial Ca^{2+} responses upon *Hrh* isoform-specific agonists in the thalamus (see Figure S3). Like in the cortex, there was a significant portion of microglia (18.2 ± 9.6/34.1%; n = 396 cells, 43 slices, 6 mice) responding to the *Hrh1*-specific agonist 2-PEA (100 μM) which was similar to thalamic responses upon histamine (p > .9999; Figure S3A,B). The *Hrh2*-specific agonist amthamine also evoked Ca^{2+} responses in a subset of ATP-responding microglia (13.4 ± 8.3/19.6%; n = 354 cells, 34 slices, 6 mice; p > .9999). Isoform-specific activation of *Hrh3* (0.0 ± 0.0/5.4%; n = 223 cells, 34 slices, 6 mice) or *Hrh4* (0.0 ± 0.0/0.0%; n = 275 cells, 37 slices, 6 mice) did not have significant effects on microglial Ca^{2+} levels in thalamus when compared with spontaneous baseline activity. To further validate these results, we tested microglial histamine responses in thalamus in the presence of *Hrh*-isoform-specific blockers (Figure S3). Strikingly, the *Hrh1*-specific antagonist cetirizine (10 μM) significantly decreased microglial Ca^{2+} responses upon histamine application (0.0 ± 0.0/14.9%; n = 244 cells, 32 slices, 5 mice; p < .0001). Antagonizing *Hrh2* by using tiotidine (10 μM) did not significantly affect histamine responses of thalamic microglia (15.5 ± 7.9/26.7%; n = 425 cells from 38 slices and 6 mice; p > .9999). Likewise, *Hrh3* (carcinine; 10 μM) had no significant effects on microglial histamine responses (18.33 ± 0/34.37%; n = 358 cells, 40 slices, 6 mice; p = > .9999; Figure S3A,B). Taken together, our data indicate the involvement of *Hrh1* and *Hrh2* in microglial histamine responses in cortex and thalamus, with *Hrh1* being more predominantly involved. These findings are in contrast to our data on isolated microglia demonstrating that *Hrh2* is the only microglia-intrinsic histamine receptor opening the possibility that the microglia *Hrh1*-mediated response could be indirect and mediated by another cell type.

3.4 | Hrh1-mediated microglial Ca^{2+} responses are indirectly mediated via astrocytes

Astrocytes express *Hrh1* receptors (Zhang et al., 2014) and were previously shown to respond with Ca^{2+} elevations to histamine via *Hrh1* (Jung et al., 2000). It suggests that they could be a potential source for signaling substances that are released in a histamine (*Hrh1*)-dependent fashion from astrocytes and sensed by microglia. We revisited the previous findings and studied astrocytic Ca^{2+} level changes in response to histamine in situ. AM-ester-coupled Ca $^{2+}$ indicators are usually nicely taken up by cultured or isolated microglia (e.g., Elmadany, de Almeida Sassi, et al., 2020; Hoffmann et al., 2003; Moller et al., 2000), however, in brain slices taken up mainly by astrocytes (Schipke et al., 2002). We confirmed this previous finding by comparing Fluo4/AM labeling with fluorescence reporter expression in acute brain slices from GFAP-RFP mice. As shown in Figure S6, Fluo4/AM signals largely overlapped with RFP fluorescence (95.9 ± 3.9%), indicating that the Ca^{2+} indicator was taken up by GFAP+ cells, putatively astrocytes. In fact, this finding does not exclude non-astrocytic cells types with a similar morphology like NG2 cells. However, NG2 glia usually do not express GFAP (Dawson, 2003) and contribute to a rather low extent (2%–3%) to the cell population of the CNS as compared with GFAP+ astrocytes (10%–15%). We therefore conclude that the majority of the Fluo4-labelled cells in our slices are astrocytes and we used this Ca^{2+} indicator for loading cortical brain slices from C57/Bl6 mice. As shown in Figure 3a,b, 76.5 ± 52.5/87.9% of the cortical ATP-responding cells displayed Ca^{2+} elevations upon external application of 100 μM histamine ($n = 143$ cells, 11 slices, 3 mice) which was significantly more than basal, spontaneous astrocytic Ca^{2+} elevations (0.0 ± 0.0/6.4%; $p = .0002$). We did the same experiment in cortical slices from Csf1r-2A-mCherry-2A-GCaMP animals (Figure S7) and discriminated microglia by their transgenic mCherry fluorescence from astrocytes (mCherry-). The response rate of the mCherry+ cells was comparable to that of microglial cells in Figure 2 (12.5 ± 5.8/20.6%; $n = 160$ cells, 12 slices, 4 mice) and was significantly smaller than the response rate of mCherry- cells (64.6 ± 42.6/88.8%; $n = 158$ cells, 14 slices, 4 mice).

The application of 2-PEA (*Hrh1 agonist*; 100 μM) led to comparable astrocytic Ca^{2+} responses (80.0 ± 66.7/88.9%; n = 124 cells, 10 slices, 3 mice; $p = .0013$ vs. basal and $p = .0013$ vs. histamine), suggesting that *Hrh1* is the dominant histamine receptor isoform in cortical astrocytes. The astrocytic response rate upon the *Hrh2*-specific agonist amthamine was 6.5 ± 0.0/20.5% ($n = 129$ cells, 11 slices, 3 mice) which was not significantly different from basal activity ($p > .9999$). We also investigated thalamic astrocytes and found—similar to cortical astrocytes—the majority of cells responding to histamine (70.7 ± 32.1/82.7%; $n = 168$ cells, 16 slices, 2 mice; Figure 3c,d) and *Hrh1* stimulation (2-PEA; 60.0 ± 39.7/79.7%; $n = 133$ cells, 13 slices, 4 mice; $p > .9999$ vs. histamine) whereas there was no response upon *Hrh2* activation (amthamine; 0.0 ± 0.0/0.0%; $n = 147$ cells, 16 slices, 4 mice; $p < .0001$ vs. histamine).

We therefore conclude that astrocytes express functional *Hrh1* receptors in cortex and thalamus being, thus, potential sources of a *Hrh1*-dependent secondary signaling toward microglial receptors.

3.5 | Microglia Ca^{2+} responses to histamine are dependent on P2ry12 signaling

It has been previously shown that purinergic signaling is a strong communication pathway between astrocytes and microglia, and that astrocytic Ca^{2+} elevations can be followed by ATP release and subsequent microglial Ca^{2+} responses (Schipke et al., 2002; Verderio & Matteoli, 2001). The data above demonstrate that astrocytes but not microglia respond to *Hrh1* stimulation. In an attempt to test for the hypothesis that *Hrh1* stimulation indirectly mediates microglial Ca^{2+} responses via astrocytes and ATP release, we blocked *P2ry12* which is specifically expressed by microglia in the brain, and which is the predominant (metabotropic) purinergic receptor in microglia (Figure 4a,b). Cortical brain slices from microglia Ca^{2+} indicator mice were incubated for 2 min with AR-C69931 (1 μM) prior to the application of histamine (100 μM). The blockade of *P2ry12* dramatically reduced microglial histamine responses to levels indistinguishable from baseline activity: only 2.70 ± 0/3.72% of ATP-responding microglia displayed histamine responses in the presence of AR-C69931 ($n = 590$ cells, 23 slices, 4 mice; $p = .6808$ vs. basal and $p = .0012$ vs. histamine/control), suggesting that ATP is the messenger that causes cortical microglial Ca^{2+} responses upon histamine application. Microglia histamine responses were also inhibited in thalamus, however, to a lower extent. In the presence of AR-C69931, 12.0 ± 4.6/16.9% of the microglia responded upon histamine application ($n = 393$ cells from 20 slices and 4 mice). This was not significantly different from spontaneous activity (0.0 ± 0.0/1.1%, $p = .6371$), but there was also no significant differences to histamine application alone (25.0 ± 11.9/45.8%, $p = .4579$).

3.6 | Histamine stimulates microglial phagocytic activity via Hrh1

To study the effect of brain histamine on microglia at a more functional level, we tested if and how microglia phagocytosis is modulated by histamine. Phagocytic activity was quantified according to our previously published in situ assay (Wendt et al., 2017). Acute brain slices from adult C57BL/6J mice were incubated for 60 min with latex beads and the number of beads incorporated into a 3D-rendered Iba1-labeled (microglia) volume was subsequently counted using confocal imaging and 3D reconstruction (Figure 5a). Per animal and condition, we quantified microglial phagocytosis in 4–5 cortical brain slices, analyzing 4–5 randomly chosen fields of view per slice by z-stacks in the cortex (layers I–VI). As shown in Figure 5b, baseline phagocytic index in the cortex (1.65 ± 0.93/2.47; $n = 54$) was significantly enhanced when histamine (100 μM) was co-applied together with the beads (2.87 ± 2.14/3.87; $n = 90$; $p < .0001$). As there was only a low percentage of cortical microglia responding to histamine with intracellular Ca^{2+} elevations (12.1 ± 5.3%/20.0%; see Figure 2a,b), we addressed the question if the increase in microglial phagocytosis upon histamine incubation could be due to a stimulation of only a subpopulation of microglial cells (Figure S4A), and therefore determined the

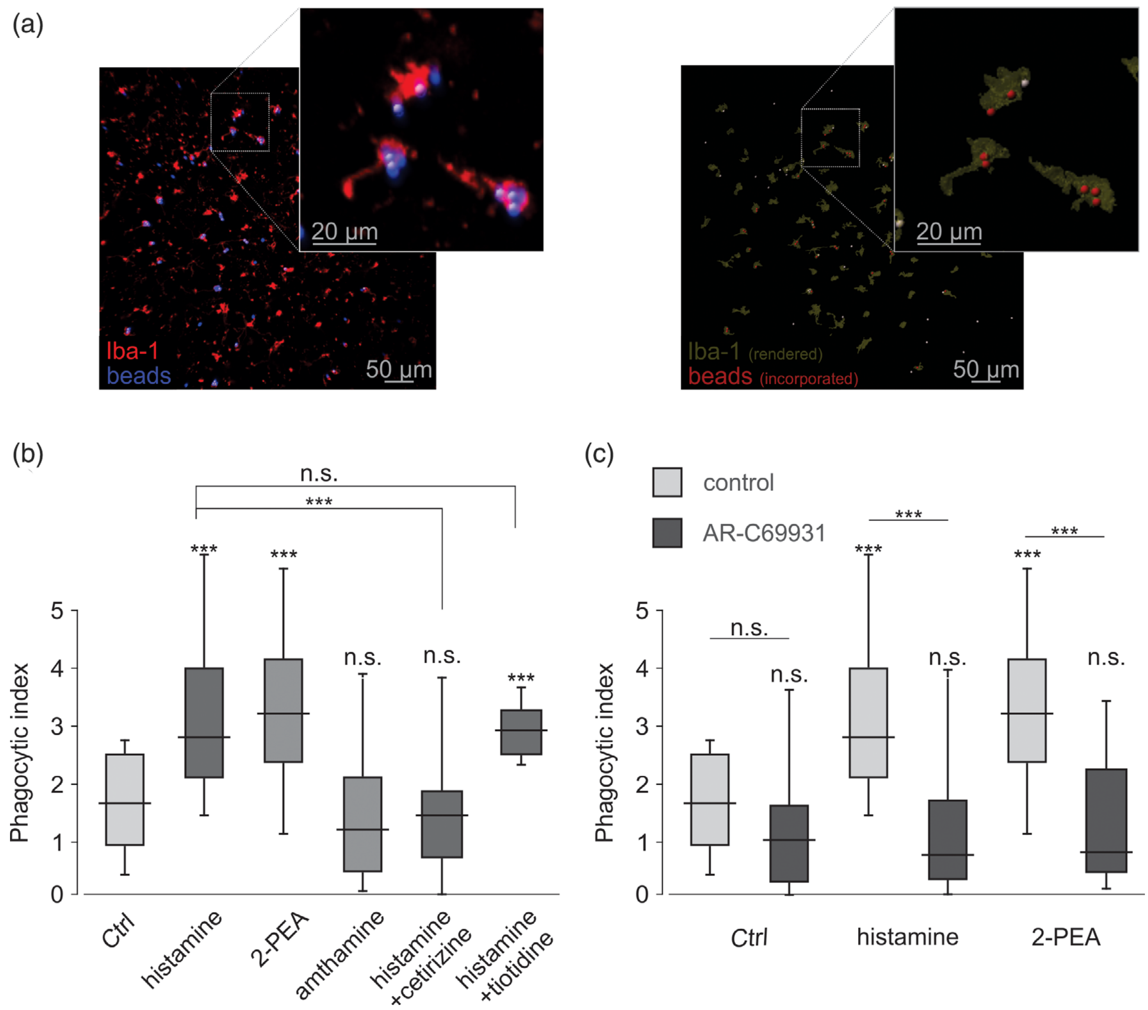

FIGURE 5 Microglial phagocytosis in the cortex is stimulated by histamine via *Hrh1* and *P2ry12*. (a) *Left*, representative confocal image of Iba1-stained cortical microglia (red) together with latex beads (blue) performed on brain slices from an adult WT male mouse. *Right*, 3D reconstruction of Iba1-positive microglia is shown with automatically counted phagocytosed beads (shown in red). Scale bars: 50 µm. The insert shows the cells at higher magnification. (b) Comparison of phagocytic activity of cortical microglia under control conditions (white), in the presence of histamine (black), in the presence of the subtype-specific histamine receptor agonists 2-PEA (*Hrh1* agonist; 100 µM gray) or amthamine (*Hrh2* agonist; 10 µM; gray) or in the presence of histamine plus the subtype-specific histamine receptor antagonists cetirizine (*Hrh1* antagonist; 10 µM; black) or tiotidine (*Hrh2* antagonist; 10 µM; black). Phagocytic index indicates the number of incorporated beads per Iba$^+$ volume (see material and methods). (c) Effect of *P2ry12* blockade (1 µM AR-C69931) on microglial phagocytic activity under control and under histamine (100 µM)- or 2-PEA (100 µM)-stimulating conditions. Box plots indicate the median (black line) as well as the 25%–75% (box) and 10%–90% (whiskers) percentiles. Statistical significance was tested by a Kruskal Wallis test followed by Dunn's multiple comparisons test and is indicated as followed: n.s., $p \geq .05$; *$p \leq .05$; **$p \leq .01$, ***$p \leq .001$. Number of mice/slices: N(Ctrl) = 6/55; N(histamine) = 6/90; N(2-PEA) = 3/34; N(amthamine) = 3/33; N(histamine+cetirizin) = 3/44; N(histamine+tiotidine) = 2/20; N(ARC) = 3/45; N(histamine+ARC) = 3/45; N(2-PEA +ARC) = 3/45

fraction of phagocyting microglia under control and histamine-stimulating conditions. Under control conditions, on average 6.7 ± 0.6 microglial cells per view field incorporated one bead, which increased to 12.3 ± 0.7 cells during histamine incubation ($p < .0001$, Figure S4A). Comparing microglial cells incorporating two or more beads under control and histamine-stimulating conditions led to a similar increase (2 beads: 1.6 ± 0.3 and 4.4 ± 0.4 microglia/VF; 3 beads: 0.5 ± 0.1 and 1.6 ± 0.2 microglia/VF; 4 beads: 0.1 ± 0.1 and 0.7 ± 0.1 microglia/VF for control and histamine, respectively; $p < .0001$ for all comparisons). As the total number of microglial cells within each scanned volume (225 µm × 225 µm × 21 µm) was 113.3 ± 4.4 (n = 144 view fields), the histamine-induced increase in phagocytosis was apparent in 9.2 ± 0.4% of the observed microglia which is in a similar range like histamine-responding microglia in Ca^{2+} imaging experiments.

Microglia Ca^{2+} responses to histamine have been similar in thalamus and cortex (see Figure S2B). We therefore tested if the stimulation of phagocytic activity by histamine is also comparable in thalamus. Interestingly, thalamic microglial phagocytosis was generally at a lower level than cortical, with a phagocytic index of 0.44

± 0.15/0.59 under control conditions ($n = 36$; p < .0001 vs. cortex, Figure S5). As in the cortex, a significant stimulation of phagocytosis occurred in the presence of histamine (1.11 ± 0.63/1.42; $n = 33$; p < .0001 vs. ctrl). The increase in phagocyting microglia was 11.5 ± 2.0%, and not significantly different from cortex ($p = .5863$).

In an attempt to further study the histamine-induced stimulation of microglial phagocytosis, we also tested the isoform-specific agonists 2-PEA (100 μM; *Hrh1*), amthamine (10 μM; *Hrh2*), R-(−)-a-methylhistamine dihydrobromide (αMH; 1 μM; *Hrh3*), or VUF 10460 (10 μM; *Hrh4*) in order to activate histamine receptors in a subtype-specific manner. Interestingly, as summarized in Figure 5b, only incubation with the *Hrh1*-specific agonist 2-PEA elevated microglial phagocytosis in cortex (3.24 ± 2.38/3.77; $n = 34$; p < .0001 and p > .9999 compared with control and histamine, respectively) whereas there was no effect when *Hrh2* were specifically activated (1.25 ± 0.48/1.93; $n = 33$; p > .9999 vs. control, Figure 5b). There was likewise no effect on phagocytosis by stimulation of *Hrh3* (1.67 ± 0.58/2.01; $n = 28$; p < .8299 vs. control, data not shown) or *Hrh4* (1.86 ± 1.41/2.26; $n = 15$; p > .9999 vs. control, data not shown). We further verified these results by blocking *Hrh1* receptors using Cetirizin dihydrochloride (5 μM) when slices were incubated with histamine. Indeed, histamine-mediated stimulation of phagocytosis was completely blocked by *Hrh1* inhibition (1.45 ± 0.73/1.81; $n = 44$; p > .9999 vs. control). The blockade of *Hrh2* by using 10 μM tiotidine did not affect cortical phagocytosis of microglia.

In thalamus, the *Hrh* subtype-specific effects on microglia phagocytic activity were similar to cortex (Figure S5B), with a stimulation by 2-PEA (*Hrh1*) that was comparable to histamine and no effects of amthamine (*Hrh2*). Furthermore, only *Hrh1*, but not *Hrh2*, inhibition prevented histamine-induced stimulation of microglial phagocytosis. Taken together, our data demonstrate that histamine stimulates microglial phagocytosis via *Hrh1*, but not by *Hrh2* activation in cortex and thalamus. Similar to acute intracellular Ca^{2+} elevations upon histamine application, histamine incubation for 1 h increased the phagocytic activity also only in a subset of microglial cells.

3.7 | Stimulation of microglial phagocytic activity by histamine is dependent on P2ry12

We finally tested if the *Hrh1*-dependent, histamine-evoked stimulation of microglial phagocytosis is dependent on putatively secondary purinergic signals. AR-C69931 was used to block microglial *P2ry12* receptors during the 1 h incubation with the beads. As shown in Figure 5c, ARC-69931 indeed completely inhibited histamine-stimulated phagocytosis in cortex. The phagocytic index in the presence of histamine together with AR-C69931 was 0.7 ± 0.28/1.61 ($n = 45$) and therefore significantly lower than with histamine alone (2.87 ± 2.14/3.99; $n = 90$; p < .0001) as well as similar to baseline phagocytic activity under control conditions (1.65 ± 0.92/2.51; $n = 54$; $p = .3631$) or in the presence of AR-C69931 alone (0.98 ± 0.29/1.56; $n = 54$; p > .9999). Similarly, the stimulating effect of the Hrh1-specific agonist 2-PEA (100 μM; 3.24 ± 2.35/4.06) was completely abolished by AR-C69931 (0.75 ± 0.43/1.92; $n = 45$; p < .0001 vs. 2-PEA alone). In thalamus, the *Hrh1*-dependent stimulation of microglia phagocytosis was also abolished by AR-C69931 (Figure S5). In the presence of the *P2ry12* blocker, histamine (0.18 ± 0.07/0.44; $n = 36$) did not potentiate microglia phagocytic activity, suggesting that the cellular and molecular mechanisms of the stimulation are not different from cortex. Taken together, our data suggest that histamine-evoked stimulation of microglial phagocytosis depends on microglial *P2ry12* receptors in cortex and thalamus.

4 | DISCUSSION

Tonic brain histamine levels are controlled by histaminergic neurons in the tuberomammillary nucleus (TMN) in a circadian fashion and have an impact on various brain pathologies. In the present study, we investigated which receptors and pathways are involved in microglial histamine responses. In freshly isolated microglia, only the *Hrh2*-specific agonist amthamine did evoke intracellular Ca^{2+} elevations while agonists of other subtypes of histaminergic receptors did not trigger responses. Furthermore, only the blockade of *Hrh2* but not of the other *Hrh* isoforms did inhibit histamine responses of isolated microglia. We therefore confirmed many previous transcriptomic observations that microglia express *Hrh2* and not histaminergic receptors of the other three subtypes on a functional level (Butovsky et al., 2014; Consortium, 2018; Grabert et al., 2016; Hickman et al., 2013; Zhang et al., 2014).

In a tissue context, namely in cortical and thalamic brain slices, the *Hrh2*-specific agonist amthamine did trigger a response, but we found also responses upon *Hrh1* activation which were even more prominent. The transcriptomic data indicate that *Hrh1* receptors are functionally expressed by the majority of astrocytes but not in microglia. The sensitivity of microglial *Hrh1* responses to the *P2ry12* inhibitor AR-C69931 strongly suggests an astrocyte to microglia communication via ATP/ADP and *P2ry12*. We assume that activation of *Hrh1* receptors in astrocytes triggers the release of ATP/ADP which stimulates intracellular Ca^{2+} elevations and phagocytic activity in microglia via activation of *P2ry12* purinergic receptors. It is well established that these receptors are prominently expressed by microglia and that activation of these receptors can stimulate phagocytosis (Elmadany, Logiacco, et al., 2020; Inoue et al., 2009; Koizumi et al., 2007). In a recent study, we found even a significant decrease in microglia phagocytic activity in the cortex of P91-P112 male and female WT mice when P2ry12 was blocked. The reason why this result could not be confirmed in the current study might be due to the different age of the mice which was only P30–P60 here. A systematic approach of this interesting issue still remains elusive.

The treatment of acute brain slices with amthamine did not affect microglial phagocytic activity, suggesting that there is only little involvement of microglia-intrinsic *Hrh2* in controlling phagocytic activity. One possible biological role for microglial *Hrh2* receptors could be that *Hrh2* expression is low and negligible under healthy conditions, but that microglia become more directly sensitive to histamine under disease conditions as suggested by results from a previous publication of our lab in which LPS treatment significantly increased microglia responses to histamine in adult cultures (Pannell et al., 2014). Another possibility would be that *Hrh2* affects other microglial properties than phagocytosis, that is, the ramification (Frick et al., 2016), or that we oversaw potential microglia histamine responses that do not affect intracellular Ca^{2+} levels (e.g., cAMP). We could also consider that histamine receptors are not evenly distributed among the surface of microglia and that *Hrh*2 receptors are located rather in microglial processes than in the soma. Our Ca^{2+} responses are, however, dominated by signals from soma. *Hrh*2 (and also *P2ry12*) receptors are known to be linked to cAMP signaling pathways, and not-like *Hrh1*- to Ca^{2+}. However, it has been previously observed that GPCRs linked to G_i or G_s proteins can also elicit intracellular Ca^{2+} elevations (Elmadany, de Almeida Sassi, et al., 2020; Kuhn et al., 2004; Pannell et al., 2014), potentially by signaling of the Gßɤ subunits in a PLC/IP_3R-dependent fashion from internal stores (Clapham, 2007). Ca^{2+} elevations downstream of *Hrh2* (Esbenshade et al., 2003) or *P2ry12* (De Simone et al., 2010; Irino et al., 2008; Jiang et al., 2017; Pausch et al., 2004) activation were previously demonstrated. We therefore suggest that microglial *Hrh2*- and *P2ry12*-dependent Ca^{2+} responses in the current study also originate from internal release. This hypothesis would fit to our data about the sparse responses to ATP or histamine in microglial thin processes which are probably not equipped with endoplasmic reticulum or other Ca^{2+} stores.

The ambient, average histamine concentration in the extracellular space of the brain is considered to be in the range of 0.5 to 2 μM (Best et al., 2017). That does not exclude that it can be significantly higher in micro-compartments and has indeed been shown to locally increase up to 20-fold under pathophysiological conditions (Haas & Panula, 2003; Panula & Nuutinen, 2013). We used in the present study a histamine concentration of 100 μM not to mimic physiological HA level changes but rather to test for the presence of functional *Hrh* isoforms on microglia and astrocytes. The physiological relevance of our data are, thus, more on the functional expression of *Hrh* isoforms and downstream cellular pathways. In the current study, we used acute brain slices from healthy, young adult mice. Previous in vivo data have shown that calcium signaling in microglia depends on brain state, the inflammatory status and the activity of surrounding neurons (Brawek & Garaschuk, 2013; Eichhoff et al., 2011; Umpierre et al., 2020; Umpierre & Wu, 2020). Although we did not investigate microglia histamine responses in vivo, it seems very unlikely that the involvement of astrocytic *Hrh1* and microglial *P2ry12* is different in the living brain. Furthermore, there could be alterations under disease conditions due to pathophysiological changes in *Hrh* or *P2ry12* receptor expression levels or altered levels of ambient histamine.

In the current study we neither demonstrated nor ruled out a functional role of microglial Ca^{2+} signaling in phagocytosis. However, stimulation of *Hrh1* which is functionally expressed on astrocytes, stimulated microglial phagocytosis in a (microglial) *P2ry12*-dependent fashion. Our data therefore indicate that astrocytes are required for histamine stimulation of microglial phagocytic activity. There are several previous reports on the impact of histamine on microglia phagocytosis; however, there is so far no evidence for a potential interaction of astrocytes in microglial responses. In fact, studies on acutely isolated or cultured microglial cells, including the relatively non-physiological cell line N9, do not contain other cell types like astrocytes as potential source of secondary messengers (Albertini et al., 2020; Barata-Antunes et al., 2017; Ferreira et al., 2012; Iida et al., 2015; Rocha et al., 2016). To the best knowledge of the authors, there are so far two studies testing the effect of histamine on microglial phagocytosis under more physiological in situ or in vivo conditions. One study showed that microglia phagocytosis was suppressed by inhibition of *Hrh3* in organotypic hippocampal brain slices. The in vivo injection of the inverse *Hrh3* agonist JNJ10181457 into the prefrontal cortex, however, did only affect the LPS stimulation of microglia phagocytic activity, but had no effect on unstimulated microglia (Iida et al., 2017). As we did in the present study not directly test for these conditions and brain regions, these data do not necessarily contradict our results and it is quite tempting to speculate about the differences to our results. Conceivable explanations for the involvement of *Hrh3* in Iida et al. (2017) might for instance be the high density of neurons in the pyramidal layers of the hippocampus. Given that *Hrh3* is mainly expressed by neurons, it seems possible that blockade of *Hrh3*could rather have inhibited a yet unknown neuron–microglia communication than acting on microglia directly. In the present study, by using in situ Ca^{2+} imaging, we did not find any evidence for functional *Hrh3* expression on cortical and thalamic microglia and the transcriptomic data do also not support that hypothesis (Figures 1d, 2d and S3C,D). In Iida et al., however, the activation of microglia in the prefrontal cortex by LPS will have changed their expression profile, which potentially lead to an upregulation of microglia-intrinsic *Hrh3*. The second in vivo study on histamine and microglia phagocytosis was performed by Rocha et al. (2016) who found that stereotactical co-injection of histamine increased microglial engulfment of phosphatidylcholine-containing liposomes in the substantia nigra, according to a stimulation of microglial phagocytic activity by histamine. This result fits well to our findings, although the interplay between histamine and astrocytes was not tested directly. It was actually demonstrated in the same study that histamine did also stimulate phagocytosis of N9 microglia cultures in a Hrh1-dependent fashion however, the comparability of N9 microglia cultures and microglia in situ or in vivo is rather poor (Butovsky et al., 2014).

A further finding of the present study is that there are significant differences in microglial responses to histamine between different brain regions. Interestingly, microglia responses increased in corpus callosum and thalamus, thus, brain regions with a larger percentage of white matter. In thalamus, there was a similar *Hrh* subtype-specific activation pattern as in the cortex, suggesting that not the microglia-intrinsic expression of Hrh isoforms but rather the microglia communication with non-microglial cells could vary between different brain regions.

Histamine acts as a modulatory neurotransmitter and is linked to the maintenance of wakefulness in the healthy brain. Abnormalities in the histaminergic system have been associated with many brain diseases like Parkinson's disease or multiple sclerosis (Panula & Nuutinen, 2013). Microglia contribute to many physiological and nearly all pathological processes in the CNS, and their ability to sense histaminergic tones or stimuli via astrocytes and *P2ry12* might have an important impact on their behavior, including phagocytosis or synaptic pruning. We therefore conclude that all histamine-related processes in the brain could be potentially linked to microglial action via purinergic pathways, and this unexpected connection might be essential for the future development of novel immune-related therapies.

ACKNOWLEDGMENTS

We thank Regina Piske, Nadine Scharek, Bastiaan Pierik, and the microscopy core facility (Advanced Light Microscopy, ALM) of the MDC Berlin for technical assistance. We also thank Dr. Ralf Kühn and Andrea Leschke from the Transgenic Core Facility of the MDC for generating the microglia indicator mouse lines. This work was supported by the Helmholtz-Gemeinschaft, Zukunftsthema "Immunology and Inflammation" (ZT-0027), and by the Einstein-Stiftung. Open Access funding enabled and organized by Projekt DEAL.

CONFLICT OF INTEREST

The authors declare that they have no conflicts of interest with the contents of the article.

DATA AVAILABILITY STATEMENT

Data tables will be shared.

ORCID

Pengfei Xia https://orcid.org/0000-0001-5086-1755
Helmut Kettenmann https://orcid.org/0000-0001-8208-0291

REFERENCES

Albertini, G., Etienne, F., & Roumier, A. (2020). Regulation of microglia by neuromodulators: Modulations in major and minor modes. *Neuroscience Letters*, *733*, 135000. https://doi.org/10.1016/j.neulet.2020.135000

Apolloni, S., Fabbrizio, P., Amadio, S., Napoli, G., Verdile, V., Morello, G., … Volonté, C. (2017). Histamine regulates the inflammatory profile of SOD1-G93A microglia and the histaminergic system is dysregulated in amyotrophic lateral sclerosis. *Frontiers in Immunology*, *8*, 1689. https://doi.org/10.3389/fimmu.2017.01689

Bader, M. F., Taupenot, L., Ulrich, G., Aunis, D., & Ciesielski-Treska, J. (1994). Bacterial endotoxin induces $[Ca^{2+}]_i$ transients and changes the organization of Actin in microglia. *Glia*, *11*(4), 336–344.

Barata-Antunes, S., Cristóvão, A. C., Pires, J., Rocha, S. M., & Bernardino, L. (2017). Dual role of histamine on microglia-induced neurodegeneration. *Biochimica et Biophysica Acta - Molecular Basis of Disease*, *1863*(3), 764–769. https://doi.org/10.1016/j.bbadis.2016.12.016

Best, J., Nijhout, H. F., Samaranayake, S., Hashemi, P., & Reed, M. (2017). A mathematical model for histamine synthesis, release, and control in varicosities. *Theoretical Biology & Medical Modelling*, *14*(1), 24. https://doi.org/10.1186/s12976-017-0070-9

Boucsein, C., Zacharias, R., Farber, K., Pavlovic, S., Hanisch, U. K., & Kettenmann, H. (2003). Purinergic receptors on microglial cells: Functional expression in acute brain slices and modulation of microglial activation in vitro. *The European Journal of Neuroscience*, *17*(11), 2267–2276.

Bowman, R. L., Klemm, F., Akkari, L., Pyonteck, S. M., Sevenich, L., Quail, D. F., … Joyce, J. A. (2016). Macrophage ontogeny underlies differences in tumor-specific education in brain malignancies. *Cell Reports*, *17*(9), 2445–2459. https://doi.org/10.1016/j.celrep.2016.10.052

Brawek, B., & Garaschuk, O. (2013). Microglial calcium signaling in the adult, aged and diseased brain. *Cell Calcium*, *53*(3), 159–169. https://doi.org/10.1016/j.ceca.2012.12.003

Butovsky, O., Jedrychowski, M. P., Moore, C. S., Cialic, R., Lanser, A. J., Gabriely, G., … Weiner, H. L. (2014). Identification of a unique TGF-beta-dependent molecular and functional signature in microglia. *Nature Neuroscience*, *17*(1), 131–143. https://doi.org/10.1038/nn.3599

Clapham, D. E. (2007). Calcium Signaling. *Cell*, *131*(6), 1047–1058. https://doi.org/10.1016/j.cell.2007.11.028

Dawson, M. R., Polito, A., Levine, J. M., & Reynolds, R. (2003). NG2-expressing glial progenitor cells: an abundant and widespread population of cycling cells in the adult rat CNS. *Molecular and Cellular Neuroscience*, *24*(2), 476–488. https://doi.org/10.1016/s1044-7431(03)00210-0

De Simone, R., Niturad, C. E., De Nuccio, C., Ajmone-Cat, M. A., Visentin, S., & Minghetti, L. (2010). TGF-beta and LPS modulate ADP-induced migration of microglial cells through P2Y1 and P2Y12 receptor expression. *Journal of Neurochemistry*, *115*(2), 450–459. https://doi.org/10.1111/j.1471-4159.2010.06937.x

Eichhoff, G., Brawek, B., & Garaschuk, O. (2011). Microglial calcium signal acts as a rapid sensor of single neuron damage in vivo. *Biochimica et Biophysica Acta*, *1813*(5), 1014–1024. https://doi.org/10.1016/j.bbamcr.2010.10.018

Elmadany, N., de Almeida Sassi, F., Wendt, S., Logiacco, F., Visser, J., Haage, V., … Semtner, M. (2020). The VGF-derived peptide TLQP21 impairs purinergic control of chemotaxis and phagocytosis in mouse microglia. *The Journal of Neuroscience*, *40*(17), 3320–3331. https://doi.org/10.1523/jneurosci.1458-19.2020

Elmadany, N., Logiacco, F., Buonfiglioli, A., Haage, V. C., Wright-Jin, E. C., Schattenberg, A., … Gutmann, D. H. (2020). Neurofibromatosis 1 - mutant microglia exhibit sexually-dimorphic cyclic AMP-dependent purinergic defects. *Neurobiology of Disease*, *144*, 105030. https://doi.org/10.1016/j.nbd.2020.105030

Esbenshade, T. A., Hee Kang, C., Krueger, K. M., Miller, T. R., Witte, D. G., Roch, J. M., … Hancock, A. A. (2003). Differential activation of dual signaling responses by human H1 and H2 histamine receptors. *Journal of Receptor and Signal Transduction Research*, *23*(1), 17–31. https://doi.org/10.1081/rrs-120018758

Ferreira, R., Santos, T., Gonçalves, J., Baltazar, G., Ferreira, L., Agasse, F., & Bernardino, L. (2012). Histamine modulates microglia function. *Journal of Neuroinflammation*, *9*, 90. https://doi.org/10.1186/1742-2094-9-90

Frick, L., Rapanelli, M., Abbasi, E., Ohtsu, H., & Pittenger, C. (2016). Histamine regulation of microglia: Gene-environment interaction in the regulation of central nervous system inflammation. *Brain, Behavior, and Immunity*, *57*, 326–337. https://doi.org/10.1016/j.bbi.2016.07.002

Grabert, K., Michoel, T., Karavolos, M. H., Clohisey, S., Baillie, J. K., Stevens, M. P., … McColl, B. W. (2016). Microglial brain region-dependent diversity and selective regional sensitivities to aging. *Nature Neuroscience*, *19*(3), 504–516. https://doi.org/10.1038/nn.4222

Haas, H., & Panula, P. (2003). The role of histamine and the tuberomamillary nucleus in the nervous system. *Nature Reviews. Neuroscience*, *4*(2), 121–130. https://doi.org/10.1038/nrn1034

Hickman, S. E., Kingery, N. D., Ohsumi, T. K., Borowsky, M. L., Wang, L. C., Means, T. K., & El Khoury, J. (2013). The microglial sensome revealed by direct RNA sequencing. *Nature Neuroscience*, *16*(12), 1896–1905. https://doi.org/10.1038/nn.3554

Hirrlinger, P. G., Scheller, A., Braun, C., Quintela-Schneider, M., Fuss, B., Hirrlinger, J., & Kirchhoff, F. (2005). Expression of reef coral fluorescent proteins in the central nervous system of transgenic mice. *Molecular and Cellular Neuroscience*, *30*(3), 291–303. https://doi.org/10.1016/j.mcn.2005.08.011

Hoffmann, A., Kann, O., Ohlemeyer, C., Hanisch, U. K., & Kettenmann, H. (2003). Elevation of basal intracellular calcium as a central element in the activation of brain macrophages (microglia): Suppression of receptor-evoked calcium signaling and control of release function. *The Journal of Neuroscience*, *23*(11), 4410–4419.

Iida, T., Yoshikawa, T., Kárpáti, A., Matsuzawa, T., Kitano, H., Mogi, A., … Yanai, K. (2017). JNJ10181457, a histamine H3 receptor inverse agonist, regulates in vivo microglial functions and improves depression-like behaviours in mice. *Biochemical and Biophysical Research Communications*, *488*(3), 534–540. https://doi.org/10.1016/j.bbrc.2017.05.081

Iida, T., Yoshikawa, T., Matsuzawa, T., Naganuma, F., Nakamura, T., Miura, Y., … Yanai, K. (2015). Histamine H3 receptor in primary mouse microglia inhibits chemotaxis, phagocytosis, and cytokine secretion. *Glia*, *63*(7), 1213–1225. https://doi.org/10.1002/glia.22812

Inoue, K., Koizumi, S., Kataoka, A., Tozaki-Saitoh, H., & Tsuda, M. (2009). $P2Y_6$-evoked microglial phagocytosis. *International Review of Neurobiology*, *85*, 159–163.

Irino, Y., Nakamura, Y., Inoue, K., Kohsaka, S., & Ohsawa, K. (2008). Akt activation is involved in $P2Y_{12}$ receptor-mediated chemotaxis of microglia. *Journal of Neuroscience Research*, *86*(7), 1511–1519.

Jiang, P., Xing, F., Guo, B., Yang, J., Li, Z., Wei, W., … Xu, J. (2017). Nucleotide transmitters ATP and ADP mediate intercellular calcium wave communication via P2Y12/13 receptors among BV-2 microglia. *PLoS One*, *12*(8), e0183114. https://doi.org/10.1371/journal.pone.0183114

Jung, S., Pfeiffer, F., & Deitmer, J. W. (2000). Histamine-induced calcium entry in rat cerebellar astrocytes: Evidence for capacitative and non-capacitative mechanisms. *The Journal of Physiology*, *3*, 549–561. https://doi.org/10.1111/j.1469-7793.2000.00549.x

Jurič, D. M., Kržan, M., & Lipnik-Stangelj, M. (2016). Histamine and astrocyte function. *Pharmacological Research*, *111*, 774–783. https://doi.org/10.1016/j.phrs.2016.07.035

Kettenmann, H., Hanisch, U. K., Noda, M., & Verkhratsky, A. (2011). Physiology of microglia. *Physiological Reviews*, *91*(2), 461–553. https://doi.org/10.1152/physrev.00011.2010

Koizumi, S., Shigemoto-Mogami, Y., Nasu-Tada, K., Shinozaki, Y., Ohsawa, K., Tsuda, M., … Inoue, K. (2007). UDP acting at P2Y6 receptors is a mediator of microglial phagocytosis. *Nature*, *446*(7139), 1091–1095. https://doi.org/10.1038/nature05704

Korvers, L., de Andrade Costa, A., Mersch, M., Matyash, V., Kettenmann, H., & Semtner, M. (2016). Spontaneous $Ca2+$ transients in mouse microglia. *Cell Calcium*, *60*(6), 396–406. https://doi.org/10.1016/j.ceca.2016.09.004

Kuhn, S. A., van Landeghem, F. K., Zacharias, R., Färber, K., Rappert, A., Pavlovic, S., … Kettenmann, H. (2004). Microglia express GABA(B) receptors to modulate interleukin release. *Molecular and Cellular Neurosciences*, *25*(2), 312–322. https://doi.org/10.1016/j.mcn.2003.10.023

Logiacco, F., Xia, P., Georgiev, S., Chang, Y.-J., Franconi, C., Ugursu, B., Wolf, S., Kühn, R., Kettenmann, H., & Semtner, M. (in press). Microglial cells sense neuronal activity indirectly via astrocyte GABA release in the postnatal hippocampus. *Cell Reports*.

Moller, T., Kann, O., Verkhratsky, A., & Kettenmann, H. (2000). Activation of mouse microglial cells affects P2 receptor signaling. *Brain Research*, *853*(1), 49–59.

Nikodemova, M., & Watters, J. J. (2012). Efficient isolation of live microglia with preserved phenotypes from adult mouse brain. *Journal of Neuroinflammation*, *9*, 147. https://doi.org/10.1186/1742-2094-9-147

Pannell, M., Szulzewsky, F., Matyash, V., Wolf, S. A., & Kettenmann, H. (2014). The subpopulation of microglia sensitive to neurotransmitters/neurohormones is modulated by stimulation with LPS, interferon-gamma, and IL-4. *Glia*, *62*(5), 667–679. https://doi.org/10.1002/glia.22633

Panula, P., & Nuutinen, S. (2013). The histaminergic network in the brain: Basic organization and role in disease. *Nature Reviews. Neuroscience*, *14*(7), 472–487. https://doi.org/10.1038/nrn3526

Passani, M. B., Bacciottini, L., Mannaioni, P. F., & Blandina, P. (2000). Central histaminergic system and cognition. *Neuroscience and Biobehavioral Reviews*, *24*(1), 107–113.

Pausch, M. H., Lai, M., Tseng, E., Paulsen, J., Bates, B., & Kwak, S. (2004). Functional expression of human and mouse P2Y12 receptors in *Saccharomyces cerevisiae*. *Biochemical and Biophysical Research Communications*, *324*(1), 171–177. https://doi.org/10.1016/j.bbrc.2004.09.034

Rocha, S. M., Saraiva, T., Cristóvão, A. C., Ferreira, R., Santos, T., Esteves, M., … Bernardino, L. (2016). Histamine induces microglia activation and dopaminergic neuronal toxicity via H1 receptor activation. *Journal of Neuroinflammation*, *13*(1), 137. https://doi.org/10.1186/s12974-016-0600-0

Sala Frigerio, C., Wolfs, L., Fattorelli, N., Thrupp, N., Voytyuk, I., Schmidt, I., … de Strooper, B. (2019). The major risk factors for Alzheimer's disease: Age, sex, and genes modulate the microglia response to Aβ plaques. *Cell Reports*, *27*(4), 1293–1306.e6. https://doi.org/10.1016/j.celrep.2019.03.099

Schipke, C. G., Boucsein, C., Ohlemeyer, C., Kirchhoff, F., & Kettenmann, H. (2002). Astrocyte $Ca2+$ waves trigger responses in microglial cells in brain slices. *The FASEB Journal*, *16*(2), 255–257. https://doi.org/10.1096/fj.01-0514fje

Tabula Muris Consortium, T. M. (2018). Single-cell transcriptomics of 20 mouse organs creates a Tabula Muris. *Nature*, *562*(7727), 367–372. https://doi.org/10.1038/s41586-018-0590-4

Thangam, E. B., Jemima, E. A., Singh, H., Baig, M. S., Khan, M., Mathias, C. B., … Saluja, R. (2018). The role of histamine and histamine receptors in mast cell-mediated allergy and inflammation: The hunt for new therapeutic targets. *Frontiers in Immunology*, *9*(1873). https://doi.org/10.3389/fimmu.2018.01873

Umpierre, A. D., Bystrom, L. L., Ying, Y., Liu, Y. U., Worrell, G., & Wu, L. J. (2020). Microglial calcium signaling is attuned to neuronal activity in awake mice. *eLife*, *9*, 9. https://doi.org/10.7554/eLife.56502

Umpierre, A. D., & Wu, L. J. (2020). How microglia sense and regulate neuronal activity. *Glia*, *69*, 1637–1653. https://doi.org/10.1002/glia.23961

Verderio, C., & Matteoli, M. (2001). ATP mediates calcium signaling between astrocytes and microglial cells: Modulation by IFN-gamma. *Journal of Immunology*, *166*(10), 6383–6391.

Vitrac, C., & Benoit-Marand, M. (2017). Monoaminergic modulation of motor cortex function. *Frontiers in Neural Circuits*, *11*, 72. https://doi.org/10.3389/fncir.2017.00072

Wendt, S., Maricos, M., Vana, N., Meyer, N., Guneykaya, D., Semtner, M., & Kettenmann, H. (2017). Changes in phagocytosis and potassium channel activity in microglia of 5xFAD mice indicate alterations in purinergic signaling in a mouse model of Alzheimer's disease. *Neurobiology of Aging*, *58*, 41–53. https://doi.org/10.1016/j.neurobiolaging.2017.05.027

Wolf, S. A., Boddeke, H. W., & Kettenmann, H. (2017). Microglia in physiology and disease. *Annual Review of Physiology*, *79*, 619–643. https://doi.org/10.1146/annurev-physiol-022516-034406

Zhang, Y., Chen, K., Sloan, S. A., Bennett, M. L., Scholze, A. R., O'Keeffe, S., … Wu, J. Q. (2014). An RNA-sequencing transcriptome and splicing database of glia, neurons, and vascular cells of the cerebral cortex. *The Journal of Neuroscience*, *34*(36), 11929–11947. https://doi.org/10.1523/JNEUROSCI.1860-14.2014

SUPPORTING INFORMATION

Additional supporting information may be found online in the Supporting Information section at the end of this article.

How to cite this article: Xia, P., Logiacco, F., Huang, Y., Kettenmann, H., & Semtner, M. (2021). Histamine triggers microglial responses indirectly via astrocytes and purinergic signaling. *Glia*, *69*(9), 2291–2304. https://doi.org/10.1002/glia.24039